Study of $B^0 \to K^{*0}\tau\tau$ at FCC-ee

Tristan Miralles - FCC Clermont group

FCC week London: 7^{th} of June

$b \to s\tau\tau$ and objectives

- Third generation couplings in quark transitions are the less-well known.
- Specific models addressing the Flavour problem(s) often provide $b \to \tau$ enhancements or modifications w.r.t. the SM $\Rightarrow$ $b \to s\tau\tau$ ($m_\tau \sim 20 m_\mu$) is a must do to sort out the BSM models [1, 2]. Problem : measuring the ν's.
- Thanks to its clear experimental environment and its ability to produce boosted b-hadrons, FCC-*ee* looks like the right place to reconstruct the ν's.
- SM : the $b \to s\tau\tau$ transition proceeds through an electroweak penguin diagram.
- Study of the rare heavy-flavoured decay $B^0 \to K^* \tau^+ \tau^-$ at FCC-*ee*[3]. SM prediction : BR=$\mathcal{O}(10^{-7})$ $\to$ not observed yet (present limit : $\mathcal{O}(10^{-3} - 10^{-4})$ [4]).

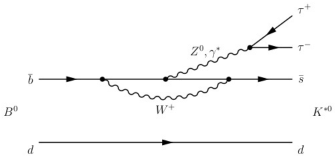

Figure – EW penguin quark-level transition

- The $B^0 \to K^*\tau\tau$ decay topology is driven by the tau decay multiplicity.
- There are from 2 to 4 neutrinos (not detected) and at least 4 charged particles in the final state and one, two or three decay vertices.
- We focus on the 3-prongs tau decays ($\tau \to \pi\pi\pi\nu$) for which the decay vertex can be reconstructed in order to solve fully the kinematics.
- 10 particles in the final state ($K, 7\pi, \nu, \bar{\nu}$), 3 decay vertices and 2 undetected neutrinos.

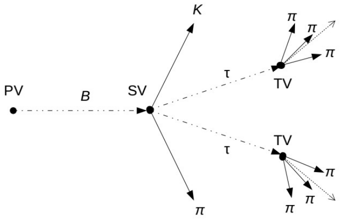

Figure – Decay topology

Goal : explore the feasibility of the search for $B^0 \to K^*\tau^+\tau^-$ and give the corresponding detector requirements.

- The events used in this work are generated with Pythia [5] ($Z \to b\bar{b}$ and hadronisation) and EvtGen [6] (forcing the decay with adequate models).
- The reconstruction is performed with the FCC Analyses sw using Delphes [7] simulation (featuring the IDEA [8] detector).
- The simulated data use particles reconstructed with the momentum resolution given by the IDEA drift chamber tracking system.
- The vertex resolutions drives the feasability of the measurement (Krakow) $\rightarrow$ the main goal of the study is to address the precision of the BF as function of the vertex resolution.
- State of the art IDEA vertexing performance will be determined and compared to other working points.

- To fully reconstruct the kinematics of the decay $\rightarrow$ neutrinos momenta must be resolved.
- Enough constraints are available in order to determine the missing coordinates.
- Energy momentum conservation at τ decay vertex $\Rightarrow$ gives the neutrino momentum at the cost of a quadratic ambiguity :

$$\begin{cases} p_{\nu_\tau}^{\perp} = -p_{\pi_t}^{\perp} \\ p_{\nu_\tau}^{\parallel} = \dfrac{((m_\tau^2 - m_{\pi_t}^2) - 2p_{\pi_t}^{\perp,2})}{2(p_{\pi_t}^{\perp,2} + m_{\pi_t}^2)} . p_{\pi_t}^{\parallel} \pm \dfrac{\sqrt{(m_\tau^2 - m_{\pi_t}^2)^2 - 4m_\tau^2 p_{\pi_t}^{\perp,2}}}{2(p_{\pi_t}^{\perp,2} + m_{\pi_t}^2)} . E_{\pi_t} \end{cases}$$

- A selection rule has to be build in order to solve the ambiguities.
- Practically energy-momentum conservation at the B decay vertex gives a condition between τ's and K^* :

$$p_{\tau^\pm} = -\frac{\vec{p}_{K*}^{\perp} . \vec{e}_{\tau^\pm}}{1 - (\vec{e}_{\tau^\pm} . \vec{e}_B)^2} - p_{\tau^\mp} . \frac{\vec{e}_{\tau^\pm} . \vec{e}_{\tau^\mp} - (\vec{e}_{\tau^\pm} . \vec{e}_B)(\vec{e}_{\tau^\mp} . \vec{e}_B)}{1 - (\vec{e}_{\tau^\pm} . \vec{e}_B)^2}$$

- Method validated at MC truth level.

- PV : 3D normal law including Beam Spot Constraints.
- SV & TV $\rightarrow$ ellipsoidal (decaying particle direction as reference) :
  - longitudinal,
  - transverse.
- Several working points examined (Longitudinal-Transverse configuration denoted as L-T in the following) :
  - 5 µm to 20 µm longitudinal,
  - 1 µm to 8 µm transverse.
- 20-3 (L-T) smearing used as reference in the following.
- Experimental vertexing efficiency is conservatively taken as 80% for the time being[i].

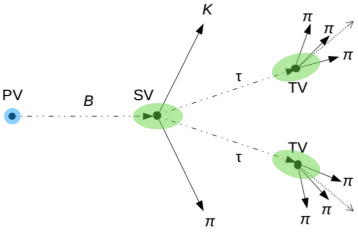

i. Due to the large multiplicity of the decay FCCAnalyses vertexing failed to estimate efficiency by itself.

- The relevant backgrounds are the ones with a similar final state than the signal ($K7\pi$).
- Several possible modes in $b \to c\bar{c}s$ and $b \to c\tau\nu$ transitions[iii] but often not observed to date $\Rightarrow$ guesstimate of the branching fraction from phase space computation and use of analogies.
- Determination of the dominant backgrounds for the measurement by building per track efficiencies from already generated ones.

iii. More details on backgrounds choices in appendix.

- The relevant backgrounds are the ones with a similar final state than the signal ($K7\pi$).
- Several possible modes in $b \to c\bar{c}s$ and $b \to c\tau\nu$ transitions [iii] but often not observed to date $\Rightarrow$ guesstimate of the branching fraction from phase space computation and use of analogies.
- Determination of the dominant backgrounds for the measurement by building per track efficiencies from already generated ones.

Decay	BF (SM/meas.)	Intermediate decay	BF_had	Additional missing particles
Signal : $B^0 \to K^*\tau\tau$	1.30×10^{-7}	$\tau \to \pi\pi\pi\nu$, $K^* \to K\pi$	9.57×10^{-11}	
Backgrounds $b \to c\bar{c}s$:				
$B^0 \to K^{*0}D_sD_s$	2.78×10^{-4}	$D_s \to \tau\nu$	5.79×10^{-10}	2ν
		$D_s \to \tau\nu, \pi\pi\pi\pi^0$	6.52×10^{-10}	ν , π^0
		$D_s \to \pi\pi\pi\pi^0$	7.35×10^{-10}	$2\pi^0$,
		$D_s \to \tau\nu, \pi\pi\pi\pi^0\pi^0$	5.47×10^{-9}	ν , $2\pi^0$
		$D_s \to \pi\pi\pi 2\pi^0$	5.17×10^{-8}	$4\pi^0$,
$B^0 \to K^{*0}D_sD_s^*$	8.78×10^{-4}	$D_s \to \tau\nu$	1.83×10^{-9}	2ν, γ/π^0
		$D_s \to \pi\pi\pi\pi^0\pi^0$	1.63×10^{-7}	$4\pi^0$, γ/π^0
Backgrounds $b \to c\tau\nu$:				
$B^0 \to K^{*0}D_s\tau\nu$	9.17×10^{-6}	$D_s \to \tau\nu$	3.59×10^{-10}	2ν
$B^0 \to K^{*0}D_s^*\tau\nu$	2.03×10^{-5}	$D_s \to \pi\pi\pi\pi^0\pi^0$	7.51×10^{-9}	$\nu, \gamma, 2\pi^0$

iii. More details on backgrounds choices in appendix.

Landscape without selection

- The B^0 mass has been reconstructed for all our modes.
- Calorimeter PID performances : π^0 detection rate of 80% is assumed in order to reduce the π^0 backgrounds.
- Backgrounds are overwhelming [iv].
- Additional selection is required. We played a Multivariate selection (XGBoost [9]).

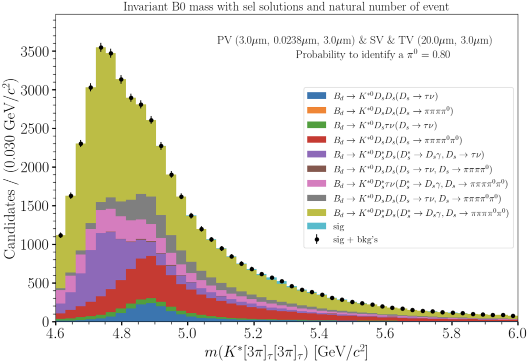

iv. Reconstruction performances for all modes in appendix.

Preselection

- Several kinematics variables has been save for each events (like momentum or intermediate mass).
- Among them several discriminatives variables have been found [v].
- The preselection has been built with these variables.
- The plot displays the result after preselection $\rightarrow$ the picture show a first improvement.
- The MVA can be trained against the backgrounds on the [5,5.6] GeV mass window.

Variable	Cut
$m^2_{2\pi\,min}$ & $m^2_{2\pi\,max}$	< 0.3 & < 0.5 GeV
p_{K*}	$<$ 1GeV
$p_{3\pi}$	$<$ 1GeV
$p_{\pi\,max}$	$<$ 0.25GeV
$p_{\pi\,min}$	$<$ 0.2GeV
FD_B	$<$ 0.3mm
FD_τ	$>$ 4mm
$m_{3\pi}$	$<$ 0.750GeV
$m_{2\pi\,max}$	$<$ 0.5GeV
$m_{2\pi\,min}$	$>$ 1GeV

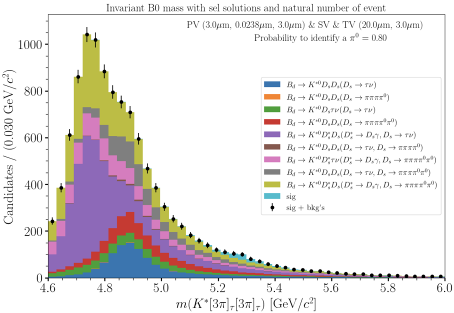

v. Example of discriminative variables in appendix.

MVA

- Training dataset generated with signal and the collection of available backgrounds.
- The backgrounds are considered in natural proportion (after the preselection).
- 50/50 split train/validation.
- Previous variables are given as inputs as well as the reconstructed p_τ of each τ candidate.
- XGB parameters optimised on AUC.
- Overtraining plot in order to check the validity of the training $\rightarrow$ OK.
- Use of the MVA [vi] to perform the selection (cut at 0.5 on the BDT output).

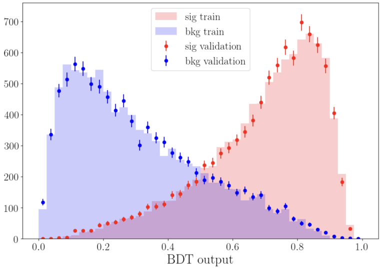

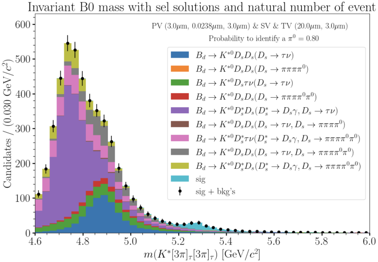

vi. Feature importance plot in appendix.

Precision of the measurement determination

- Same selection applied to other vertex resolution emulations.
- Unbinned ML fit of the data with :
  - signal → double CB + a Gaussian,
  - background → two decreasing exponential.
- Baseline : fit of the simulated signal then fit of the signal and background rescaled together.
- Extraction of the signal yield N and the associated error σ_N.
- Plot of the naive precision σ_N/N of the BF measurement of $B^0 \to K^{*0}\tau\tau$ as function of the resolution [vii].

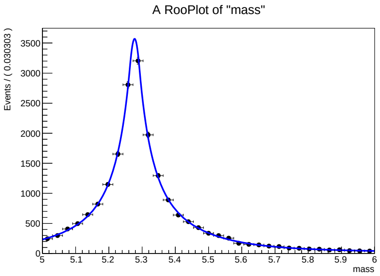

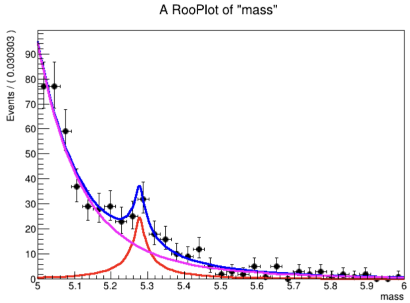

vii. Points from other longitudinal resolutions in appendix.

Precision of the measurement determination

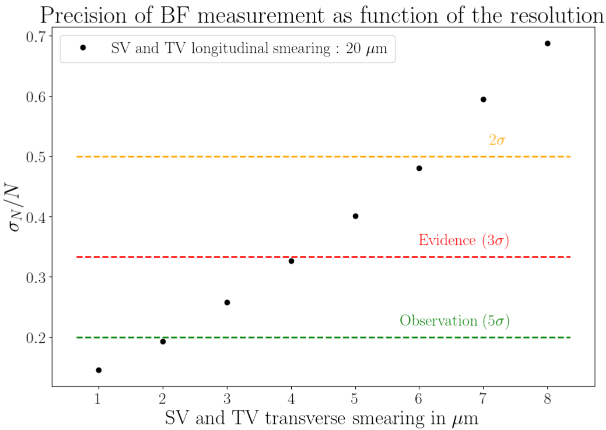

- Precision on BF measurement for fully emulated vertexing working points have been determined.
- Let's confront this to an actual state of the art vertex detector we have at hand → the IDEA vertex detector.

- Resolutions determined from 10^6 signal events.
- Reconstructed PV position fitted from reconstructed tracks with the FCCAnalyses VertexFitterSimple tools (Beam Spot Constraints set at $(4.5, 20e^{-3}, 300)$mm).
- Displacement of the reconstructed PV w.r.t. the MC truth PV is build in cartesian coordinates.
- The IDEA resolution is determined for each coordinate by a fit of the displacement :
  - double gaussian model on (x,z) [viii],
  - simple gaussian model on y.
- Resolutions $\mathcal{O}(3\,\mu\text{m})$ for (x,z).
- Resolution $\mathcal{O}(20\,\text{nm})$ for y.

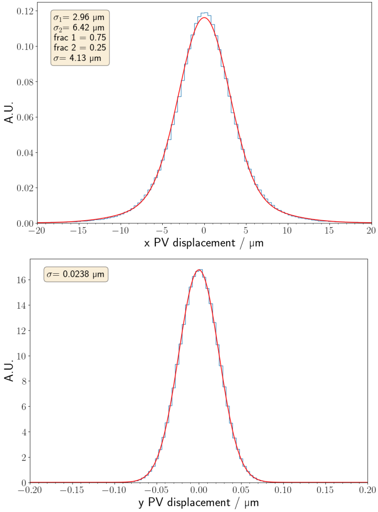

Figure – PV displacement and fit of the resolution for x (top) and y (bottom).

viii. In appendix.

The IDEA working point : secondary and tertiary vertices resolutions

- Reconstructed SV ($K^{*0} \to K\pi$) and TV ($\tau \to 3\pi$) positions fitted from MC matched reconstructed tracks via FCCAnalyses VertexFitterSimple tools.
- Displacement of the reconstructed SV and TV w.r.t. to the MC truth projected on decay plan (L-T).
- The IDEA resolution is determined for each coordinate by a fit of the displacement :
  - triple gaussian model on L,
  - simple CB model on T.
- The performances are a bit better [ix] on the TV (3 tracks) comparing to the SV (2 tracks) despite the lower daughters momenta on average.

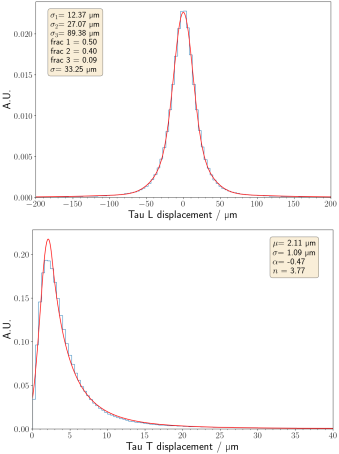

Figure – TV displacement and fit of the resolution for L (top) and T (bottom), T not signed because there is no reference T direction (not as it is in our smearing).

ix. In appendix.

- Emulation of the PV resolutions with 3D-gaussian smearing that follow the combined σ of the fits among each axis.
- SV and TV smearing via the IDEA fitted resolutions.
- Smearing emulated on each direction via accept/reject algorithms.
- SV and TV L smeared from there respective pdf's.
- SV and TV T smeared from an opportunistic 3 gaussians pdf ($\mu = 0, \sigma_1 = 2.7\,\mu\text{m}, f_1 = 50\%, \sigma_2 = 7\,\mu\text{m}, f_2 = 40\%, \sigma_3 = 20\,\mu\text{m}, f_3 = 10\%$), which reproduce approximately the IDEA T displacement distribution when emulated in 2D on the transverse plan.

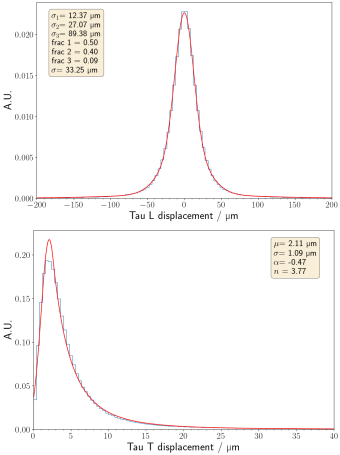

Figure – TV displacement and fit of the resolution for L (top) and T (bottom), T not signed because there is no reference T direction (not as it is in our smearing).

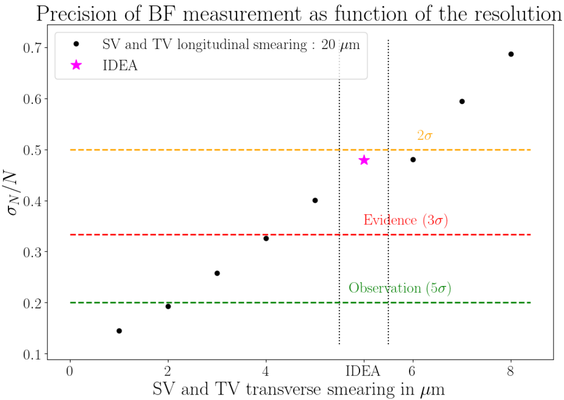

Emulation of the vertex resolution performances in order to look for the feasibility of the search of $B^0 \rightarrow K^{*0}\tau\tau$ at FCC-*ee* :

- we can't make that mode with the state-of-the-art vertex[x] detector,
- we are not that far neither.

x. **Because of a previous bug, the performance shown for IDEA has changed comparing to the one presented by Michele on Monday.**

Last projection and outlook

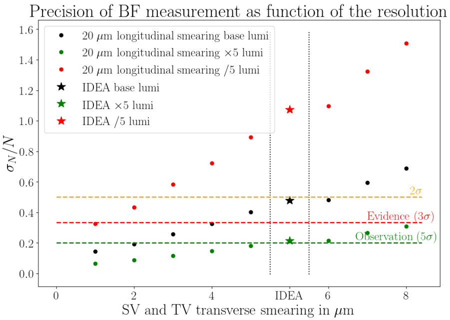

Figure – Precision on the BF measurement as function of the vertex resolution. Previous points are shown with the baseline luminosity and two other luminosity hypothesis are tested. Increasing the data taking period by a factor 5 could bring us near the observation with IDEA as it is.

Last projection and outlook

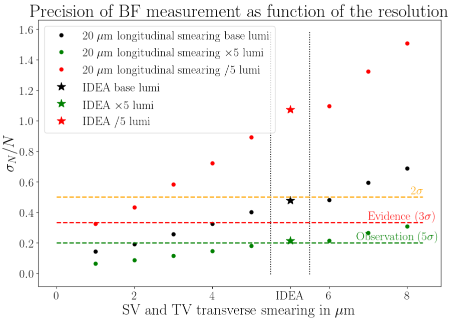

Figure – Precision on the BF measurement as function of the vertex resolution. Previous points are shown with the baseline luminosity and two other luminosity hypothesis are tested. Increasing the data taking period by a factor 5 could bring us near the observation with IDEA as it is.

- Analysis aimed at assessing the required vertexing performances to measure $B^0 \to K^{*0}\tau\tau$ from the two $\tau \to 3\pi$ self-contained method only.
- Considering τ leptonic decays on one branch of the B^0 decay brings a factor 7 in statistics. Less experimental handles but still way out to get out the signal.
- Considering fully τ leptonic decays in both branches brings a factor 14 in statistics (Impact Parameter resolution will be instrumental here)

Last projection and outlook

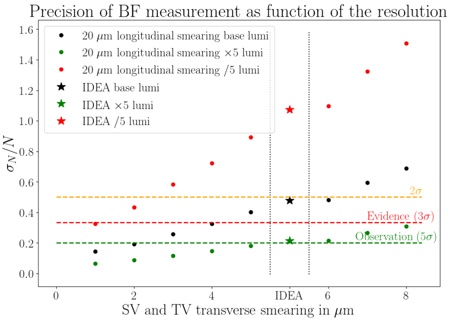

Figure – Precision on the BF measurement as function of the vertex resolution. Previous points are shown with the baseline luminosity and two other luminosity hypothesis are tested. Increasing the data taking period by a factor 5 could bring us near the observation with IDEA as it is.

- Analysis aimed at assessing the required vertexing performances to measure $B^0 \to K^{*0}\tau\tau$ from the two $\tau \to 3\pi$ self-contained method only.
- Considering τ leptonic decays on one branch of the B^0 decay brings a factor 7 in statistics. Less experimental handles but still way out to get out the signal.
- Considering fully τ leptonic decays in both branches brings a factor 14 in statistics (Impact Parameter resolution will be instrumental here)

Thanks !

To fully reconstruct the kinematics of the decay (B invariant-mass observable for instance) we need :

- Momentum of all final particles including not detected neutrinos.
- The decay lengths (6 constraints) together with the tau mass (2 constraints) can be used to determine the missing coordinates (6 degrees of freedom).
- We use energy-momentum conservation at tertiary (or τ decay) vertex with respect to τ direction [xi].

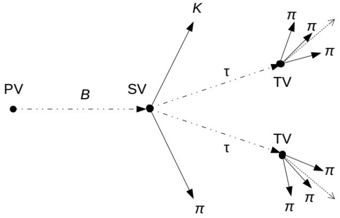

Figure – The dotted lines represent the non-reconstructed particles. The plain lines are the particles that can be reconstructed in the detector.

$$\begin{cases} p^{\perp}_{\nu_\tau} = -p^{\perp}_{\pi_t} \\ p^{\parallel}_{\nu_\tau} = \dfrac{((m^2_\tau - m^2_{\pi_t}) - 2p^{\perp,2}_{\pi_t})}{2(p^{\perp,2}_{\pi_t} + m^2_{\pi_t})}.p^{\parallel}_{\pi_t} \pm \dfrac{\sqrt{(m^2_\tau - m^2_{\pi_t})^2 - 4m^2_\tau p^{\perp,2}_{\pi_t}}}{2(p^{\perp,2}_{\pi_t} + m^2_{\pi_t})}.E_{\pi_t} \end{cases}$$

xi. Another way to do this computation is given by [10].

There is a quadratic ambiguity on each neutrino momentum !

→ The ambiguities propagate to τ and B reconstructions

→ 4 possibilities by taking all +/- combination for the two neutrinos

⇒ A selection rule is needed to choose the right possibility

⟶ From the energy-momentum conservation at the B decay vertex, we have a condition between the 2 taus and the K^* with respect to the B direction :

$$p_{\tau^+_-} = -\frac{\vec{p}^{\perp}_{K*}.\vec{e}_{\tau^+_-}}{1-(\vec{e}_{\tau^+_-}.\vec{e}_B)^2} - p_{\tau^-_+}.\frac{\vec{e}_{\tau^+_-}.\vec{e}_{\tau^-_+} - (\vec{e}_{\tau^+_-}.\vec{e}_B)(\vec{e}_{\tau^-_+}.\vec{e}_B)}{1-(\vec{e}_{\tau^+_-}.\vec{e}_B)^2}$$

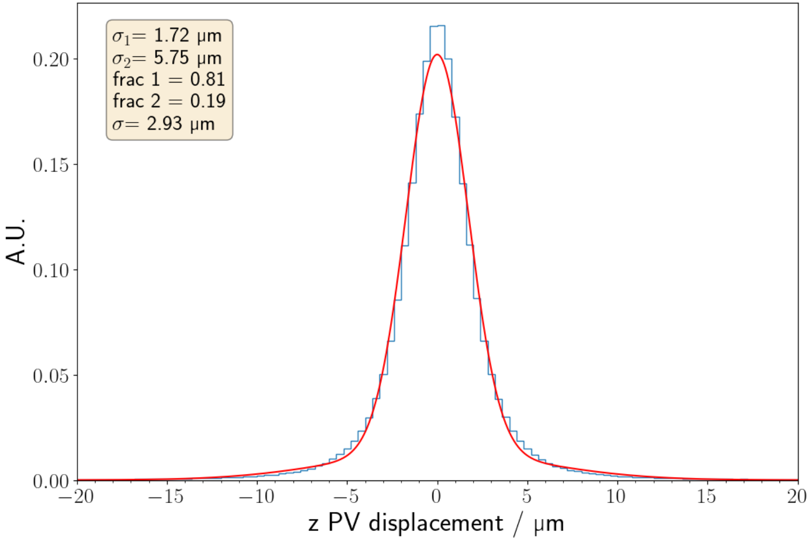

Figure – PV displacement and fit of the resolution for z

Other IDEA resolution plots

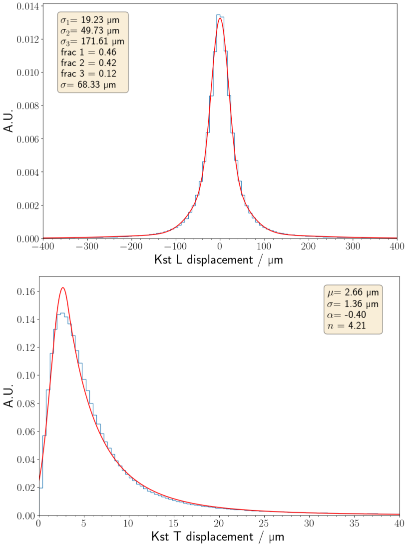

Figure – SV displacement and fit of the resolution for L (top) and T (bottom).

The knowledge of the reconstruction efficiency allows us to compute the expected number of B^0 decays fully reconstructed at FCC-*ee* :

$$\mathcal{N}_{K^*\tau\tau\to K7\pi2\nu} = \mathcal{N}_Z.BR(Z \to b\bar{b}).2f_d.BR(K^*\tau\tau).BR(\tau \to \pi\pi\pi\nu)^2.BR(K^* \to K\pi).\epsilon_{reco}.\epsilon_{vertex}$$

Where :

- $\mathcal{N}_Z = 8 \times 10^{12}$ the expected number of Z produced,
- $BR(Z \to b\bar{b}) = 0.1512 \pm 0.0005$,
- $f_d = 0.407 \pm 0.007$ the hadronisation term,
- $BR(K^*\tau\tau) = 1.30 \times 10^{-7} \pm 10\%$ the SM predicted branching fraction,
- $BR(\tau \to \pi\pi\pi\nu) = 0.0931 \pm 0.0005$,
- $BR(K^* \to K\pi) = 0.69$,
- $\epsilon_{reco} = 0.3840 \pm 0.0007$ for a smearing $3\,\mu m - 20\,\mu m$,
- $\epsilon_{reco} = 0.2850 \pm 0.0005$ for a smearing that follows IDEA performances,
- $\epsilon_{vertex} = 0.8$,

$$\Rightarrow \mathcal{N}_{K^*\tau\tau\to K7\pi2\nu} \approx 235 \pm 24 \text{ for } 20 - 3$$
$$\Rightarrow \mathcal{N}_{K^*\tau\tau\to K7\pi2\nu} \approx 175 \pm 18 \text{ for IDEA}$$

- $B^0 \to K^{*0} D_s D_s$ from analogy game :

$$BF(B^0 \to K^{*0} D_s D_s) = BF(B^0 \to DD_s) \times \frac{BF(B^0 \to D_s \pi K^0)}{BF(B^0 \to D\pi)}$$

  where $B^0 \to DD_s$ is the equivalent mode without $s\bar{s}$ from vaccum, $B^0 \to D\pi$ is the equivalent mode without $s\bar{s}$ from vaccum and with $W \to \bar{u}d$, $B^0 \to D_s \pi K^0$ is the equivalent mode with $W \to \bar{u}d$.

- $B^0 \to K^{*0} D_s^* D_s$ and $B^0 \to K^{*0} D_s^* D_s^*$ w.r.t. $B^0 \to K^{*0} D_s D_s$ from $B_s^0 \to D_s^{(*)} D_s^{(*)}$ hierarchy.
- $B^0 \to K^{*0} D_s^{(*)} \tau\nu$ from analogy via phase space computation[10] :

$$BF(B^0 \to K^{*0} D_s^{(*)} \tau\nu) = BF(B^+ \to K D_s^{(*)} \ell\nu) \times \frac{PS(B^0 \to K^{*0} D_s^{(*)} \tau\nu)}{PS(B^+ \to K D_s^{(*)} \ell\nu)}$$

  where PS denotes the Phase Space computed numerricaly (three body decay hypothesis used conservatively) and $B^+ \to K D_s^{(*)} \ell\nu$ is a reference mode with a known BF.

- $B^0 \to K^{*0} D_s \tau\nu$ and $B^0 \to K^{*0} D_s^* \tau\nu$ w.r.t $B^0 \to K^{*0} D_s^{(*)} \tau\nu$ from $B^0 \to D^{(*)} \ell\nu$ hierarchy.

- $B_s^0 \to K^{*0} D^{(*)} \tau\nu$ from analogy via phase space computation[10] :

$$BF(B_s^0 \to K^{*0} D^{(*)} \tau\nu) = BF(B_s^0 \to D_{s1}\mu\nu) \times \frac{PS(B_s^0 \to K^{*0} D^{(*)} \tau\nu)}{PS(B_s^0 \to D_{s1}\mu\nu)}$$

  where PS denotes the Phase Space computed numerricaly (three body decay hypothesis used conservatively) and $B_s^0 \to D_{s1}\mu\nu$ is a reference mode with a known BF.
- $B_s^0 \to K^{*0} D \tau\nu$ and $B_s^0 \to K^{*0} D^* \tau\nu$ w.r.t. $B_s^0 \to K^{*0} D^{(*)} \tau\nu$ from $B^0 \to D^{(*)} \ell\nu$ hierarchy.

Decay	BF (SM/meas.)	Intermediate decay	BF_had	Additional missing particles
Signal : $B^0 \to K^* \tau\tau$	1.30×10^{-7}	$\tau \to \pi\pi\pi\nu$, $K^* \to K\pi$	9.57×10^{-11}	
Backgrounds $b \to c\bar{c}s$:				
$B^0 \to K^{*0} D_s D_s$	2.78×10^{-4}	$D_s \to \tau\nu$	5.79×10^{-10}	2ν
		$D_s \to \tau\nu, \pi\pi\pi\pi^0$ xii	6.52×10^{-10}	ν , π^0
		$D_s \to \pi\pi\pi\pi^0$ xii	7.35×10^{-10}	$2\pi^0$,
		$D_s \to \tau\nu, \pi\pi\pi\pi^0\pi^0$	5.47×10^{-9}	ν , $2\pi^0$
		$D_s \to \pi\pi\pi 2\pi^0$ xii	5.17×10^{-8}	$4\pi^0$,
$B^0 \to K^{*0} D_s D_s^*$	8.78×10^{-4}	$D_s \to \tau\nu$	1.83×10^{-9}	2ν, γ/π^0
		$D_s \to \tau\nu, \pi\pi\pi\pi^0$	2.06×10^{-9}	ν , π^0, γ/π^0
		$D_s \to \pi\pi\pi\pi^0$	2.32×10^{-9}	$2\pi^0$, γ/π^0
		$D_s \to \pi\pi\pi\pi^0\pi^0$	1.63×10^{-7}	$4\pi^0$, γ/π^0
$B^0 \to K^{*0} D_s^* D_s^*$	9.10×10^{-4}	$D_s \to \tau\nu$	1.90×10^{-9}	2ν, $2\gamma/\pi^0$
		$D_s \to \tau\nu, \pi\pi\pi\pi^0$	2.14×10^{-9}	ν , π^0, $2\gamma/\pi^0$
		$D_s \to \pi\pi\pi\pi^0$	2.41×10^{-9}	$2\pi^0$, $2\gamma/\pi^0$
Backgrounds $b \to c\tau\nu$:				
$B_s \to K^{*0} D\tau\nu$	7.27×10^{-5}	$D \to \pi\pi\pi\pi^0$	1.65×10^{-9}	ν, π^0
$B_s \to K^{*0} D^*\tau\nu$	2.03×10^{-4}	$D^* \to D^0\pi, D\pi^0$		
		$D \to \pi\pi\pi\pi^0$	1.12×10^{-9}	ν, $2\pi^0$
		$D^0 \to 2\pi 2\pi\pi^0$	8.98×10^{-10}	ν, $2\pi^0$, $2\pi^\pm$
$B^0 \to K^{*0} D_s\tau\nu$	9.17×10^{-6}	$D_s \to \tau\nu$	3.68×10^{-10}	2ν
		$D_s \to \pi\pi\pi\pi^0$	4.15×10^{-10}	ν, π^0
$B^0 \to K^{*0} D_s^*\tau\nu$	2.03×10^{-5}	$D_s \to \tau\nu$	8.07×10^{-10}	2ν, γ/π^0
		$D_s \to \pi\pi\pi\pi^0$	9.09×10^{-10}	ν, π^0, γ/π^0
		$D_s \to \pi\pi\pi\pi^0\pi^0$	7.51×10^{-9}	ν, γ, $2\pi^0$

xii. $D_s \to 3\pi n\pi^0$ modes involves η/ω intermediate states (see appendix).

Better simulations for $D_s \to \pi\pi\pi n\pi^0$

- Previously this decay has been generated in the Phase Space $\to$ a more accurate simulation of the decay is needed $\Rightarrow$ new samples which include η/ω (saturating the inclusive BF) intermediate states are in order.
- Replacement of the previous samples.
- $B^0 \to K^{*0} D_s D_s (D_s \to \pi\pi\pi\pi^0)$ is now $B^0 \to K^{*0} D_s D_s$ where $D_s \to \eta/\omega\pi$ and $\eta/\omega \to \pi\pi\pi^0$.
- $B^0 \to K^{*0} D_s D_s (D_s \to \pi\pi\pi\pi^0\pi^0)$ is now $B^0 \to K^{*0} D_s D_s$ where $D_s \to \eta/\omega\pi\pi^0$ and $\eta/\omega \to \pi\pi\pi^0$.

Distribution of π^0 momentum from $D_s \to 3\pi 2\pi^0$

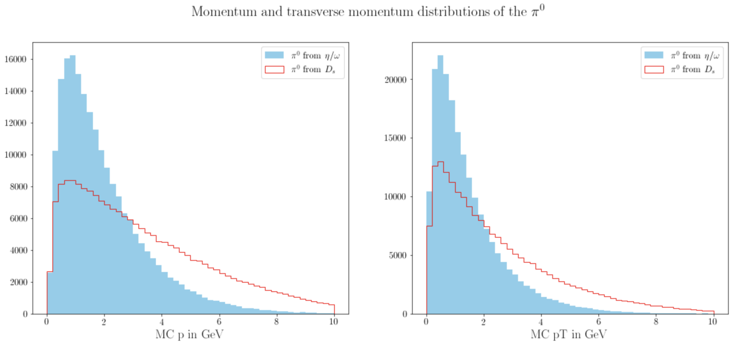

Figure – Distribution of π^0 momentum from $D_s \to 3\pi 2\pi^0$.

- $B^0 \to K^{*0} D_s D_s$ with the two D_s deacying as $D_s \to \tau\nu$, $D_s \to \pi\pi\pi\pi^0$ and $D_s \to \pi\pi\pi\pi^0\pi^0$ already generated.
- $B^0 \to K^{*0} D_s^* D_s$ with the two D_s deacying as $D_s \to \tau\nu$ already generated.
- $B^0 \to K^{*0} D_s D_s$ with both $D_s \to \tau\nu$ and $D_s \to \pi\pi\pi\pi^0$ already generated.
- Construction of a "per track" efficiency by taking the square root of the reconstruction efficiency of the four first modes $\Rightarrow \epsilon(D_s \to \tau\nu)$, $\epsilon(D_s^* \to \tau\nu)$, $\epsilon(D_s \to \pi\pi\pi\pi^0)$ and $\epsilon(D_s \to \pi\pi\pi\pi^0\pi^0)$.
- Cross check : $\epsilon(D_s \to \tau\nu) \times \epsilon(D_s \to \pi\pi\pi\pi^0) \simeq \epsilon(B^0 \to K^{*0} D_s D_s, D_s \to \tau\nu, D_s \to \pi\pi\pi\pi^0)$.
- Construction of an $\epsilon(*) = \epsilon(D_s^* \to \tau\nu)/\epsilon(D_s \to \tau\nu)$.
- Computation of an estimated efficiency for the possible background from these per track efficiencies.
- Ranking of the backgrounds via $BF \times \epsilon$.
- Choice of the biggest one for each type of specific topology.

Reconstruction efficiency

Data	Reconstruction 20 − 3
$B^0 \to K^{*0}\tau\tau(\tau \to \pi\pi\pi\nu)$	0.3840 ± 0.0007
$B^0 \to K^{*0}D_sD_s(D_s \to \tau\nu)$	0.4749 ± 0.0004
$B^0 \to K^{*0}D_sD_s(D_s \to \pi\pi\pi\pi^0)$	0.02190 ± 0.00002
$B^0 \to K^{*0}D_sD_s(D_s \to \pi\pi\pi\pi^0, \tau\nu)$	0.1014 ± 0.0001
$B^0 \to K^{*0}D_sD_s(D_s \to \pi\pi\pi\pi^0\pi^0)$	0.5630 ± 0.0005
$B^0 \to K^{*0}D_s\tau\nu(D_s \to \tau\nu)$	0.4285 ± 0.0004
$B^0 \to K^{*0}D_s^*D_s(D_s^* \to D_s\gamma, D_s \to \tau\nu)$	0.4827 ± 0.0004
$B^0 \to K^{*0}D_s^*\tau\nu(D_s^* \to D_s\gamma, D_s \to \pi\pi\pi\pi^0\pi^0)$	0.4726 ± 0.0004
$B^0 \to K^{*0}D_sD_s(D_s \to \tau\nu, \pi\pi\pi\pi^0\pi^0)$	0.5164 ± 0.0004
$B^0 \to K^{*0}D_s^*D_s(D_s^* \to D_s\gamma, D_s \to \pi\pi\pi\pi^0\pi^0)$	0.5730 ± 0.0004

Reconstructed p_{tau} distribution signal vs backgrounds 20 − 3 configuration

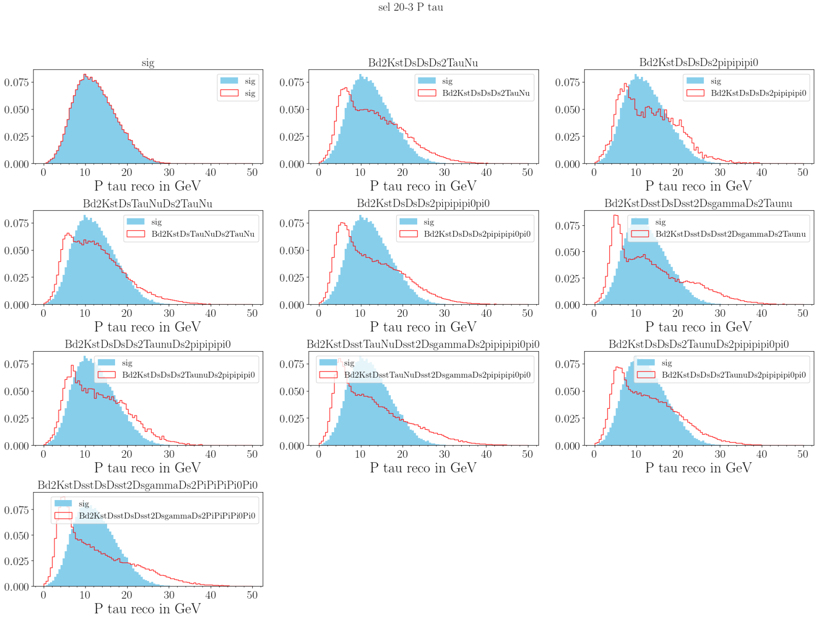

FD_τ distribution signal vs backgrounds 20 — 3 configuration

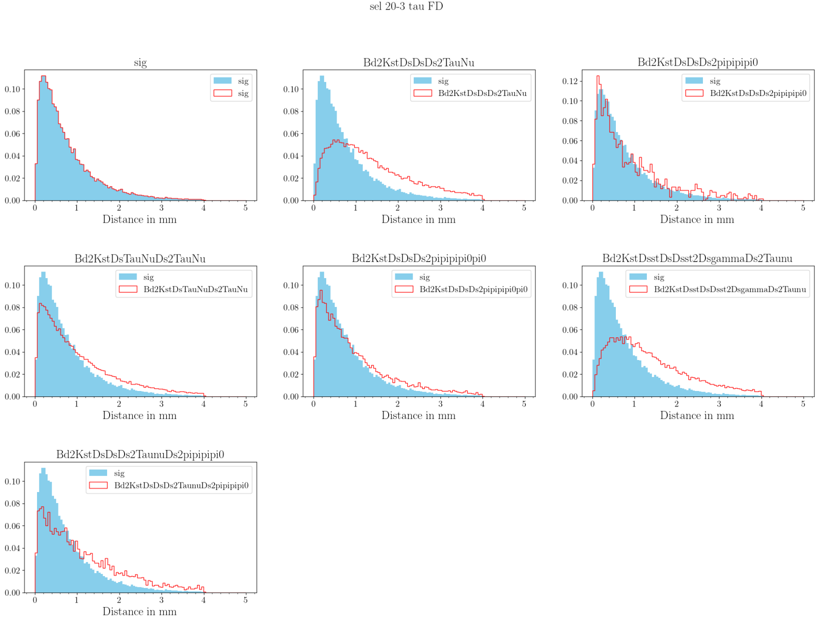

Dalitz plane (, $m^2_{\pi_{max}}$, $m^2_{\pi_{min}}$) signal and backgrounds 20 — 3 configuration

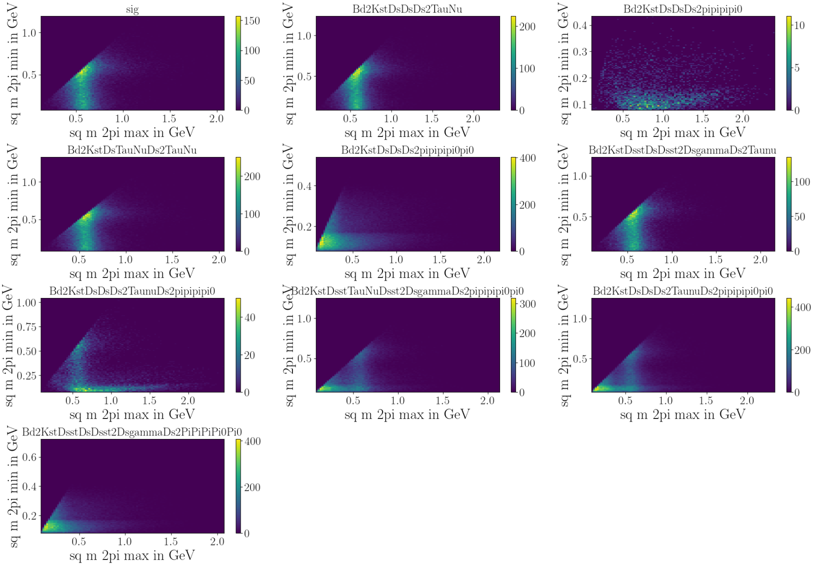

XGB features importances

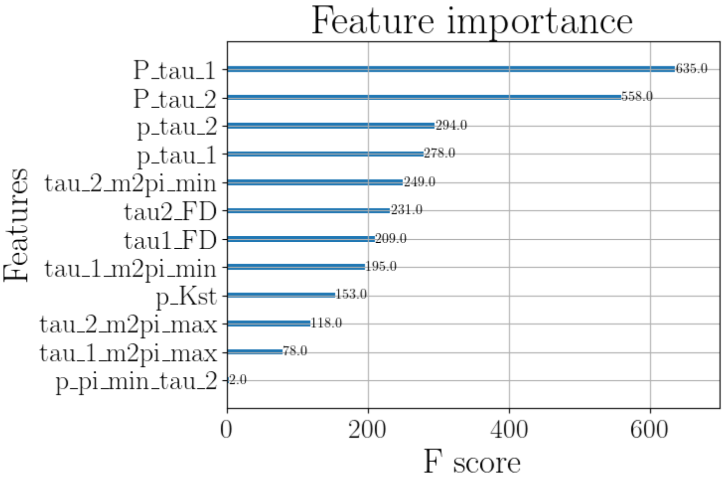

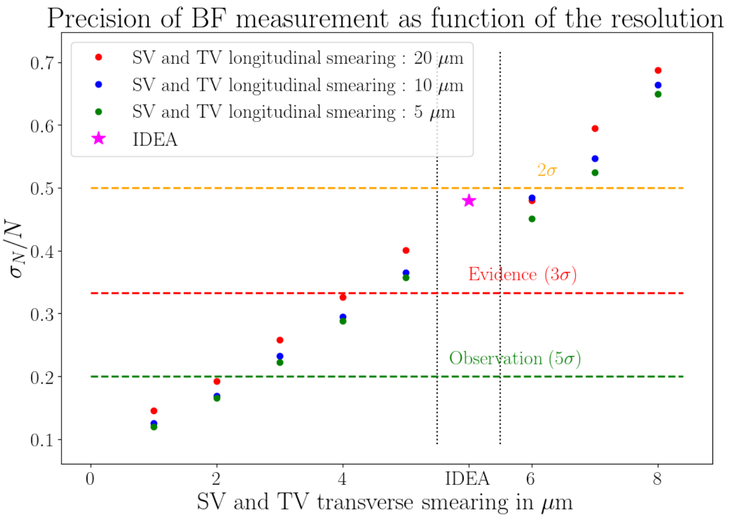

Figure – Precision on the BF measurement as function of the vertex resolution with 3 longitudinal configurations. Observed hierarchy issue comes from the interplay between the smearing of the vertexing and the fit model.

Paul Langacker.
The physics of heavy z' gauge bosons.
Reviews of Modern Physics, 81(3) :1199, 2009.

I Dorsner, S Fajfer, A Greljo, JF Kamenik, and N Kosnik.
Physics of leptoquarks in precision experiments and at particle colliders.
Physics Reports, 641 :1–68, 2016.

JF Kamenik, S Monteil, A Semkiv, and L Vale Silva.
Lepton polarization asymmetries in rare semi-tauonic $b \to s$ b$\to$ s exclusive decays at fcc-ee.
The European Physical Journal C, 77(10) :1–19, 2017.

BABAR Collaboration et al.
Search for b+-> k+ tau (+) tau (-) at the babar experiment.
Physical Review Letters, 2017, vol. 118, num. 3, p. 031802, 2017.

Torbjörn Sjöstrand, Stefan Ask, Jesper R Christiansen, Richard Corke, Nishita Desai, Philip Ilten, Stephen Mrenna, Stefan Prestel, Christine O Rasmussen, and Peter Z Skands.
An introduction to pythia 8.2.
Computer physics communications, 191 :159–177, 2015.

Anders Ryd, David Lange, Natalia Kuznetsova, Sophie Versille, Marcello Rotondo, DP Kirkby, FK Wuerthwein, and A Ishikawa.
Evtgen : a monte carlo generator for b-physics.
BAD, 522 :v6, 2005.

J De Favereau, Christophe Delaere, Pavel Demin, Andrea Giammanco, Vincent Lemaitre, Alexandre Mertens, Michele Selvaggi, Delphes 3 Collaboration, et al.
Delphes 3 : a modular framework for fast simulation of a generic collider experiment.
Journal of High Energy Physics, 2014(2) :57, 2014.

CERN.
2nd fcc-france workshop, jan 20-21, 2021.
https:...Physics.pdf.

Tianqi Chen and Carlos Guestrin.
Xgboost : A scalable tree boosting system.
In *Proceedings of the 22nd acm sigkdd international conference on knowledge discovery and data mining*, pages 785–794, 2016.

Lingfeng Li and Tao Liu.
$b \to s\tau + \tau$- physics at future z factories.
Journal of High Energy Physics, 2021(6) :1–31, 2021.